Looking on the bright side of photomask imaging

Markus benk,*[a] Chaoying Gu,[b] Rohan Karthik,[c] Daniel Vega,[c]
Kenneth Goldberg,[a] Bruno La Fontaine[a]
[a]Lawrence Berkeley National Laboratory, 1 Cyclotron Road, Berkeley, CA, 94720, USA;
[b]Department of Electrical Engineering and Computer Sciences, University of California, Berkeley, 253 Cory Hall, Berkeley, CA, 94704, USA;
[c]Inversion Semiconductor, Inc., 2261 Market Street, STE 22326 San Francisco, CA 94114, USA

ABSTRACT

Advanced mask metrology tools play a key role in research and development towards future nodes of EUV lithography. Experimental studies are an essential complement to simulation data in photomask technology and lithographic imaging. We are commissioning a mask-imaging demonstrator powered by a high-brightness undulator light source at beamline twelve of the Advanced Light Source at Lawrence Berkeley National Laboratory. The instrument is a zoneplate-based actinic full-field EUV microscope similar to the SHARP microscope, enabling complementary imaging modes, increasing the photon flux at the mask by two orders of magnitude. At frame rates above one hundred hertz, more than a thousand individual pupil channels can be recorded per experiment site, resolving the source-angular spectrum produced by the illuminator. Arbitrary pupil fills can be synthesized from the image data. The data can be used to compute Fourier-Ptychographic reconstructions. Fourier Ptychography (FP) is a computational imaging technique that reconstructs the complex field of the object from a series of intensity images recorded under plane-wave illumination from different illumination angles. FP enables quantitative phase imaging. FP data can be used to emulate wafer-side through-focus behavior in anamorphic image data. We provide an overview of the instrument, discuss data acquisition modes, and present a range of image data, demonstrating short exposure times, FP, and source optimization.

Keywords: SHARP, mask imaging, photomask, Fourier Ptychography, EUV lithography

1. INTRODUCTION

Actinic mask imaging tools for review[1] and inspection[2] typically use plasma sources with non-directional emission characteristics. Beam sources with directional emission characteristics are also used in photomask imaging.[3] Sources using high-harmonics generation[4] (HHG) achieve high brightness numbers, but the in-band EUV power and the achievable photon flux at the sample for this type of source is limited. Accelerator-based sources[5] have directional emission characteristics. These sources achieve high levels of brightness and higher photon flux at the sample than HHG sources. Accelerator-based sources are larger than plasma sources and HHG-sources. They require radiation shielding. While the etendue of plasma sources exceeds the etendue of a mask imaging tool, the etendue of a beam source is a closer match. Beam sources can therefore be integrated in mask imaging tools efficiently.

The Sharp Hyper-NA Actinic Reticle review Project[6] (SHARP) is an actinic, synchrotron-based, full-field EUV mask microscope operating at bend-magnet beamline 11.3.2 at the Advanced Light Source at Lawrence Berkeley National Laboratory. The instrument uses zoneplate lenses as imaging optics. The microscope achieves a full-well exposure time of three seconds at 0.33 4xNA, the mask-side equivalent of the 0.33NA generation of EUV lithography. For applications where a higher throughput is desired, a reduction in exposure time can be achieved through changes to the tool architecture, or by using a higher-brightness light source. The Center for X-Ray Optics operates a number of branchlines of undulator beamline twelve at the Advanced Light Source. Branchline 12.0.1.3 is equipped with focusing optics in a Kirkpatrick-Baez[7] (KB) configuration. The focus distance and beam divergence can be adjusted, changing the curvature of the bendable mirrors. A photon flux of $7 \cdot 10^{12}$ photons per second within a bandwidth $\lambda/\Delta\lambda$ of 1000 is measured at the beamline intermediate focus at 13.5-nm wavelength.

*mpbenk@lbl.gov

Photomask Technology 2026, edited by Vicky Philipsen, Vidya Vaenkatesan,
Proc. of SPIE Vol. 14273, 142730P · 2026 Published by SPIE
0277-786X · doi: 10.1117/12.3119695

The beamline intermediate focus at SHARP's bend magnet beamline 11.3.2 measures about 150µm FWHM. The divergence of the beam is less than 2.5 mrad. Adjusting the KB mirrors of the undulator branchline to similar beam characteristics would require a conjugate distance of a few meters between the KB mirror pair and the beamline focus. Due to spatial constraints at the beamline, the available conjugate distance is limited to 1.2 m. At this conjugate distance, the intermediate focus of the undulator branchline measures about 30µm FWHM. Based on the acceptance angles of the KB mirrors, the beam divergence is up to 6.7 mrad in the vertical direction and up to 12 mrad in the horizontal direction. The far-field beam profile has not been measured, but the angular extent of the beam is expected to be smaller than the acceptance angles of the KB mirrors.

2. MASK-IMAGING DEMONSTRATOR

To evaluate photomask imaging at a high-brightness undulator beamline and to assess achievable exposure times, a mask-imaging demonstrator is installed at the branchline. The demonstrator uses the SHARP illuminator optics and zoneplates, as well as the image sensor. Some of the components are removed from the SHARP microscope temporarily. Other components used in the demonstrator are spare parts for the SHARP microscope, as well as some obsolete microscope components. The demonstrator uses a compact vacuum chamber with a built-in three-axis stage, originally designed for a project that has since been completed. To tie the components together, a lid with a SHARP-specific geometry is fabricated for the vacuum chamber. The scope of the project is to operate the demonstrator for a few weeks to record image data. Due to the approaching extended shutdown of the synchrotron facility, the project has to be completed within about six months. While the demonstrator is optically identical to the SHARP microscope, it is as a temporary setup built under time and budget constraints. It does not have the mechanical stability, vibration isolation, beam diagnostics and alignment aides, complex software, automation and mask handling of the SHARP microscope. The demonstrator achieves adequate image quality, but some of the aforementioned limitations impact the imaging performance of the instrument.

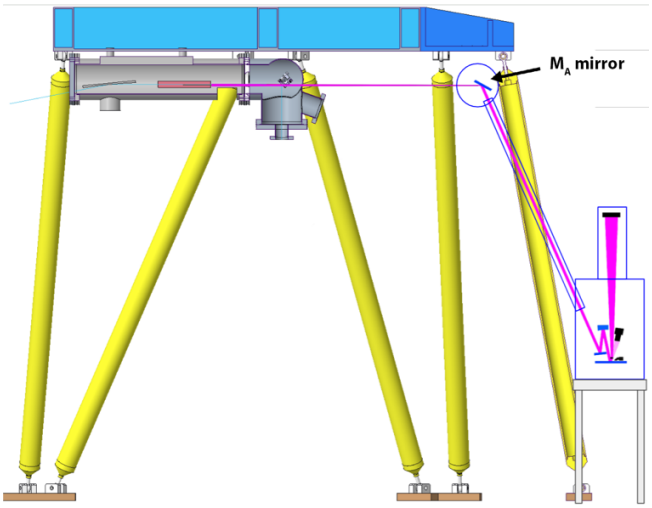


Figure 1. Sketch of the final section of the undulator branchline, showing the tank and support structure with the beamline focusing-mirrors, mirror M_A, the components of the microscope demonstrator, and the ray path to the image sensor.

A sketch of the final section of the beamline with the mask-imaging demonstrator is presented in Figure 1. The synchrotron light is focused on flat turning mirror Ma. An ellipsoidal illuminator mirror reimages the beamline focus from mirror M_A onto the photomask in critical illumination, at a demagnification of 10x. A flat folding mirror is installed between M_A and the illuminator mirror for practical reasons. A zoneplate lens above the photomask projects the image onto a CMOS image sensor. The zoneplate has a working distance of 500 µm. The magnification is 900x. The SHARP microscope is equipped with a variety of zoneplates with different mask-side aperture shapes and sizes, and a variety of imaging modes. All image data recorded on the mask-imaging demonstrator use 0.33 4xNA zoneplates.

Mirror M_A is a two-axis scanning mirror with a diameter of 1.2 mm. The mirror scans the synchrotron light across the aperture of the illuminator mirror at frequencies up to one kHz. To produce the desired pupil fill, mirror M_A scans the corresponding pattern across the angular space over the course of the exposure. SHARP's bend-magnet beamline has slits to control the angular extent of the unscanned beam. The undulator beamline has a fixed-size aperture that can be used to reduce the angular extent of the beam roughly by a factor three. The angular extent of the beam affects pupil resolution and image contrast. Due to significant spatial coherence across the beam, an increase in divergence of the unscanned beam does not correspond to an increase in pole size in a system using an incoherent light source. To increase the uniformity of the illumination across the field of view, the illuminator mirror can also be scanned, steering the illuminator focus across the mask surface by a few microns during the exposure.

The SHARP illuminator has been designed for an exposure time of a few seconds. Standard pupil fills take about 0.5 seconds to scan. The illuminator design is not suitable for exposure times far below 0.5 seconds. A fly's-eye illuminator[8] illuminates the photomask from all illumination angles at the same time, instead of scanning a beam across the angular space. This type of illuminator is well-suited for an instrument designed to provide flexible control of the pupil fill and short exposure times at the same time. Using such an illuminator would add significant cost and complexity to the instrument.

Figure 2 a shows an image of larger contacts on clear multilayer, recorded on the microscope demonstrator. The field of view is 5.7 µm at the mask. The diffraction-limited central imaging region of the microscope is about 4 µm by 4 µm. The exposure time of the image is 20 milliseconds. At the center, the exposure level is close to the full-well capacity of the image sensor. Figure 2 b shows an image of the same pattern, where the illuminator mirror is scanned to produce a more uniform central image region. The image is also recorded at a 20-ms exposure time. The uniformity scan reduces the exposure level to one third of the full-well capacity, corresponding to a 60-ms full-well exposure time. Both images are recorded using the static beam, not scanning the M_A mirror. Figure 2 c shows an image of 20-nm CD (wafer scale, 1x) lines on clear multilayer. While standard pupil fills take 0.5 seconds to scan, a simpler pupil fill, in this case a high-sigma annular fill can be scanned within a few milliseconds. The image has 17k counts at an exposure time of 30 milliseconds, corresponding to a full-well exposure time of about 100 milliseconds.

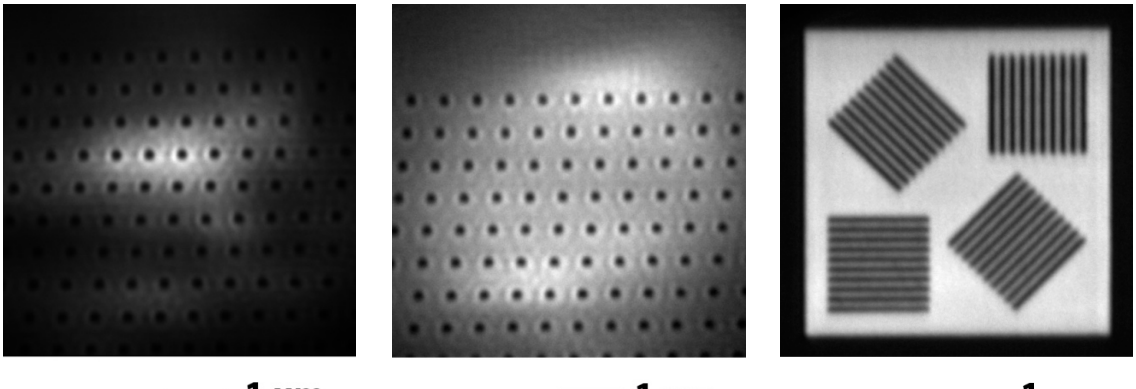


Figure 2. Image of large contacts on clear multilayer, recorded without a uniformity scan (a), image of the same pattern, recorded with a uniformity scan (b), and image of 20-nm CD (1x) lines on clear multilayer, recorded using a high-sigma annular pupil fill and uniformity scan (c).

3. SOURCE ANGULAR STACK

Initially, the SHARP microscope had been equipped with a CCD image sensor with a low frame rate and significant readout time. The microscope has since been upgraded with a faster CMOS image sensor. In 16-bit imaging mode, the image sensor reads out the full array of 2048 by 2048 pixels at a frame rate of up to 24 frames per second. Reading out a smaller region of interest corresponding to the diffraction-limited central imaging region of the microscope, frame rates of up to 300 frames per second are available in 12-bit mode.

The default imaging mode of the SHARP microscope is to synthesize the desired pupil fill scanning the beam across the aperture of the illuminator mirror over the course of the exposure, integrating the image contributions from the range of illumination angles on the image sensor. The fast CMOS sensor enables an additional imaging mode, where instead of integrating over the contributions from the different illumination angles, separate images are recorded for all illumination angles across the pupil at a high frame rate. Instead of taking images with a given pupil fill, a dataset is recorded that can later reproduce the corresponding image for any desired pupil fill. The partially coherent image is the linear combination of images from the stack that correspond to the illumination angles that form the pupil fill.

At a framerate of 300 hertz, 1500 pupil channels can be recorded in five seconds. Such short data acquisition times enable through-focus data collection. The individual images from the stack have a low exposure level and significant shot noise. If the combined exposure time of the stack is higher than the exposure time of a regular SHARP image, synthesized images from the stack will have levels of shot noise similar to a regular SHARP image. In order to synthesize images corresponding to pupil-fill ratios down to 10%, the combined exposure time of the stack should be ten times the exposure time of a regular SHARP image. At the bend-magnet beamline, both the framerate of the camera and the flux at the photomask limit the achievable data acquisition time. At the undulator beamline, achievable data acquisition times are mostly limited by the framerate of the image sensor.

A stack of 1500 images is recorded on the SHARP microscope at the bend-magnet beamline. Figure 3 a shows a single image from the stack. The mask pattern consists of 20 nm CD (1x) lines on clear multilayer in four different orientations. The exposure time is ten milliseconds per image, corresponding to a total exposure time of 15 seconds, which is about four times longer than the exposure time of a regular SHARP image. The acquisition time for the stack exceeds the total exposure time by a few seconds due to additional readout time. The exact burden depends on the size of the region of interest. The image in Figure 3 a has a maximum exposure level of 300 counts. Another stack of 1500 images is recorded at an exposure time of 50 milliseconds per image. The stack has lower shot noise. At 50 milliseconds, the acquisition time of the stack is impractical for routine data collection. Figure 3 b shows an image from the stack. The image has up to 1200 counts. The total exposure time of the stack is 75 s.

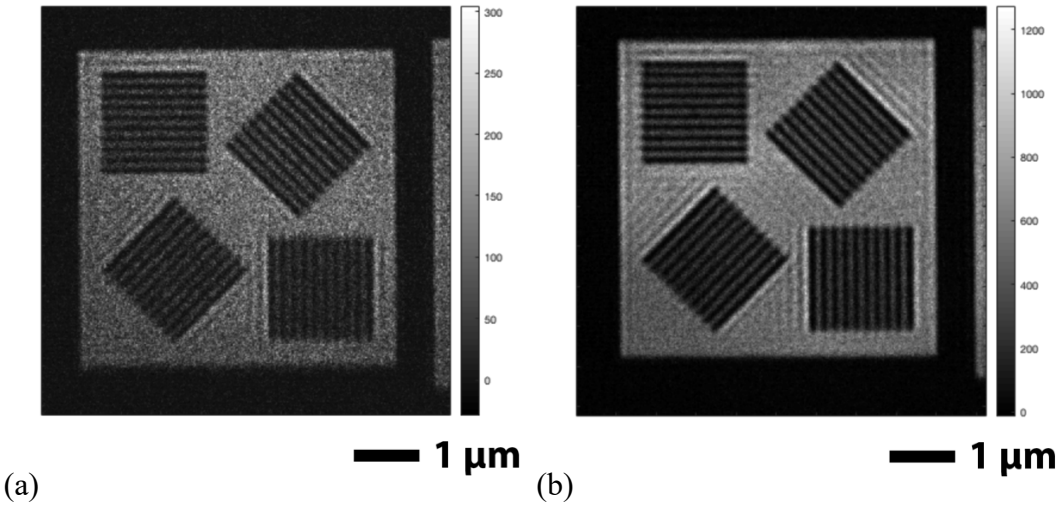


Figure 3. Image of 20 nm CD (1x) lines on clear multilayer, recorded at an exposure time of ten milliseconds (a), and image of the same pattern, recorded at an exposure time of 50 milliseconds.

Figure 4 shows image data synthesized from the stack with the 10-ms exposure time, and the corresponding pupil fill for each image. The images with the low pupil-fill-ratio (PFR) dipole illumination have a maximum exposure level of 14k to 18k counts, which is less than the typical 50k to 60k counts of a regular SHARP image. The image with the small conventional pupil fill has 55k counts, matching a regular SHARP image. The image with the high-sigma annular pupil fill has 200k counts, which is higher than the exposure level of a regular SHARP image. The synthesized images have the same contrast as regular SHARP image data recorded with the corresponding pupil fill.

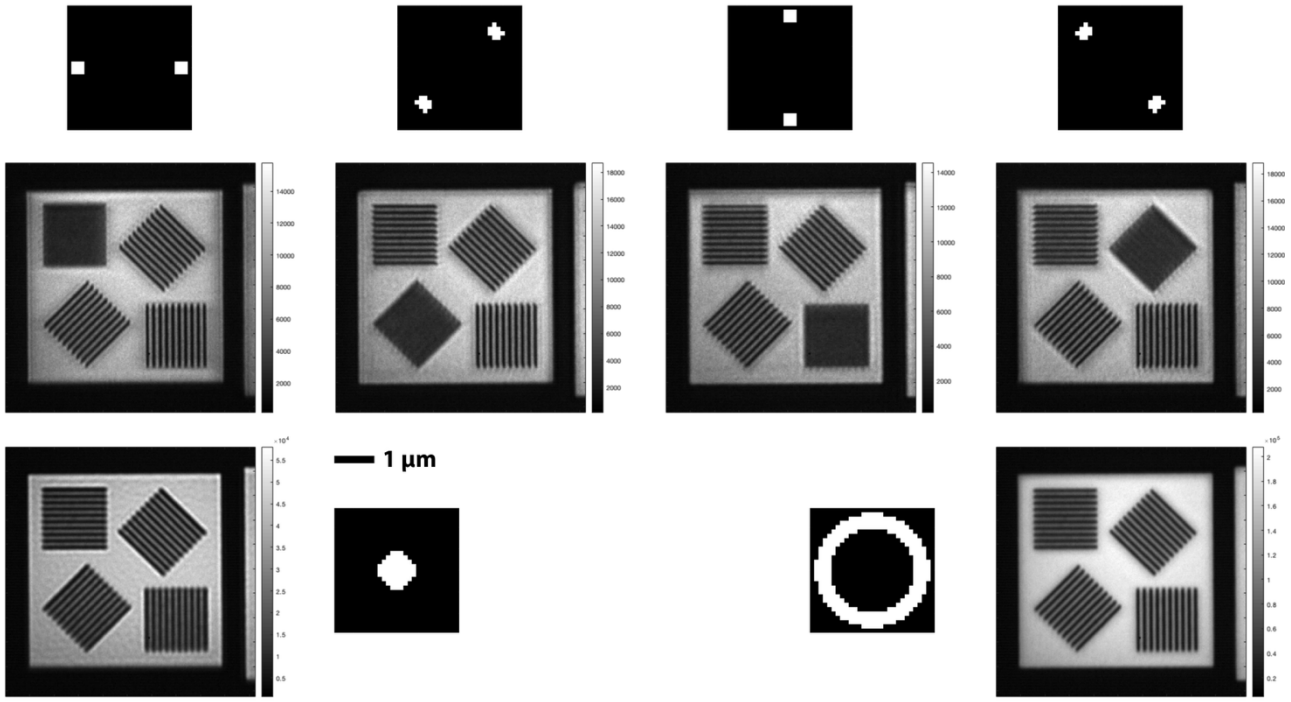


Figure 4. Synthetic images of 20-nm CD (1x) lines on clear multilayer, computed from the source angular stack with the 10-ms exposure time, and corresponding pupil fills.

Stacks of images resolving the source angular spectrum are also recorded on the mask-imaging demonstrator at the undulator beamline. Figure 5 shows synthetic images of 27.5 nm (1x) contacts, computed for four different pupil fills. The stack contains image data recorded at 1000 illumination angles. The exposure time is five milliseconds per image. The total acquisition time is eight seconds. All synthetic images have peak exposure levels of 400k counts per pixel or above. The corresponding pupil fills are shown above the images.

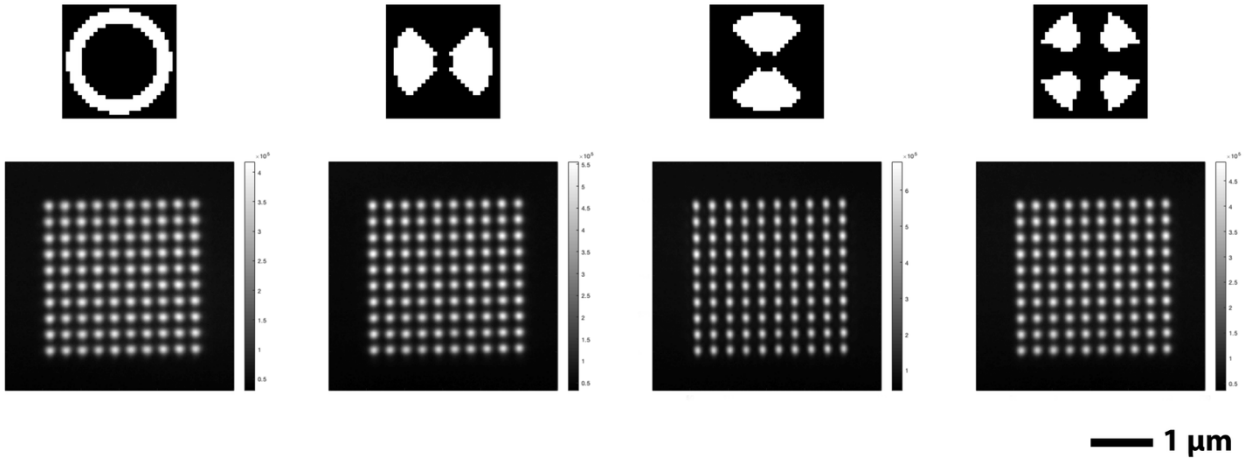


Figure 5. Synthetic images of 27.5 nm (1x) contacts, computed from a source angular stack with a 5-ms exposure time, recoded at the undulator beamline, and corresponding pupil fills.

To increase the accuracy of the technique, stacks of 1000 images are recorded at the undulator beamline, using an aperture that decreases the divergence of the unscanned beam to a level similar to the bend-magnet beamline. The exposure time is 20 ms per image. Figure 6 shows synthetic images of 15 nm CD (1x) line ends with a gap of 22.5 nm (1x), computed for four different pupil fills. The peak exposure level reaches 200k counts, or above, for all images. The data illustrate how different parts of the source angular spectrum affect different parts of the pattern.

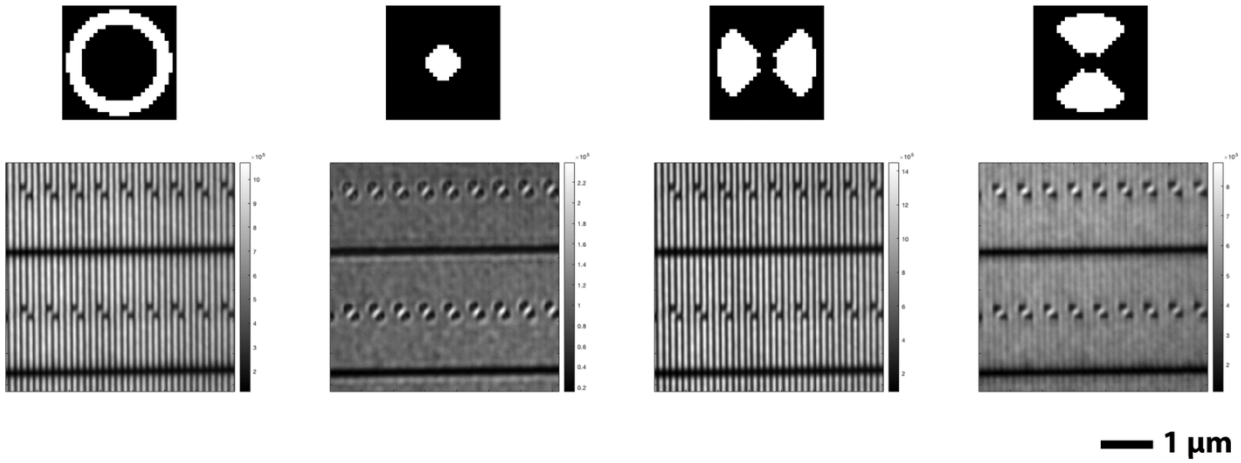


Figure 6. Synthetic images of 15 nm CD (1x) line ends with a gap of 22.5 nm (1x), computed from a source angular stack with a 20-ms exposure time, recoded at the undulator beamline, and corresponding pupil fills.

4. FOURIER PTYCHOGRAPHIC IMAGING

Fourier Ptychography (FP) is a computational imaging technique that reconstructs the complex field of the object from a series of intensity images recorded under different illumination angles. Fourier Ptychography enables quantitative phase imaging and pupil-fill synthesis. FP data can be used to scale anamorphic image data in the Fourier domain and emulate wafer-side through-focus behavior. FP is a routinely-used complementary imaging mode on the SHARP microscope. The standard FP dataset on SHARP has 37 illumination angles, uniformly spaced across the zoneplate aperture. An exposure time of a few seconds per image is used. Except for the difference in exposure time, an FP dataset is just a subset of the source angular stack presented in section 3. Being able to compute FP reconstructions from the source angular stack adds additional capabilities to the imaging mode. While shot noise in a single image is a concern, the total number of detected photons in the stack is much higher than in a regular FP dataset. There is a range of algorithmic options to compute FP reconstructions from the stack, which will be thoroughly evaluated with respect to overall performance and robustness to shot noise.

To establish a baseline, FP reconstructions are computed using image data taken from the stacks shown in Figure 3. The intensity reconstruction, computed from 37 random images from the stack with the 10-ms exposure time, is presented in Figure 7 a. The reconstruction has adequate uniformity and modulation. High-spatial-frequency granularity is visible, which is not typically found in FP reconstructions using image data with a multi-second exposure time. The coefficient of variation (CV) is 0.14 on the clear-multilayer region in the center of the pattern. Figure 7 d shows a synthetic image, computed from the FP reconstruction. The image corresponds to a vertical-dipole pupil fill at 40% PFR, as shown in Figure 6. Summing up the contributions from all illumination angles that are part of the pupil fill, and filtering by the aperture eliminate the granularity. In the image, the intensity variation on the clear multilayer matches roughness-induced variation observed in regular SHARP images recorded using partially coherent illumination. Figure 7 b shows an FP reconstruction using 37 random images from the stack with the 50-ms exposure time. The reconstruction looks similar to Figure 7 a. The CV is 0.14 also. Figure 7 c shows an FP reconstruction from the stack with the shorter 10-ms exposure time, using 75 random images instead of 37. The reconstruction shows a slight reduction in granularity, with a CV of 0.12. These initial findings suggest that FP reconstruction from the angular stack are feasible. Further investigation is needed to minimize the impact of shot noise on the reconstruction.

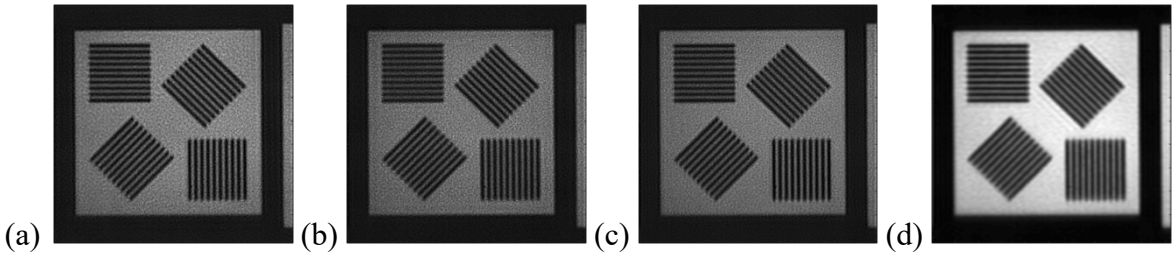


Figure 7. FP reconstruction (intensity), computed using 37 random images from the source angular stack with the 10-ms exposure time (a), FP reconstruction (intensity), computed using 37 random images from the source angular stack with the 50-ms exposure time (b), FP reconstruction (intensity), computed using 75 random images from the source angular stack with the 10-ms exposure time (c), and synthetic image, computed from FP reconstruction a, using vertical-dipole illumination at 40% PFR.

5. SOURCE OPTIMIZATION

Source mask optimization (SMO) is commonly used to increasing printability, process window, and yield for patterning at low k1 factors. SMO relies on simulation. Subtle differences between a photomask and the model, e.g., complex refractive index, film thickness, absorber sidewall angle, can significantly impact the aerial image.[9] The SHARP microscope has been used to experimentally verify the imaging performance of freeform pupil fills on an actual photomask.

As a complement to SMO, the source angular stack can be used to compute source optimizations, directly using image data from a real photomask with all of its physical properties. To illustrate the idea, the source angular stack shown in Figure 6 is used. The optimization algorithm minimizes the edge-placement error between the ideal pattern and the aerial image at a threshold. The optimization follows an approach presented in Reference 10. To improve printability of the horizontal jog, a small region of interest is selected, containing roughly the same length of horizontal and vertical edges. Figure 8 shows a smaller region of the 15 nm CD (1x) line ends with a gap of 22.5 nm (1x) from Figure 6. The optimization starts from a sigma one disk illuminator (b). The corresponding image (a) has breaks in the horizontal jogs at threshold. Image (d) corresponds to the optimized source (c). It has increased LER and CD variation for the 15 nm CD (1x) lines and spaces, but does not have any breaks at threshold.

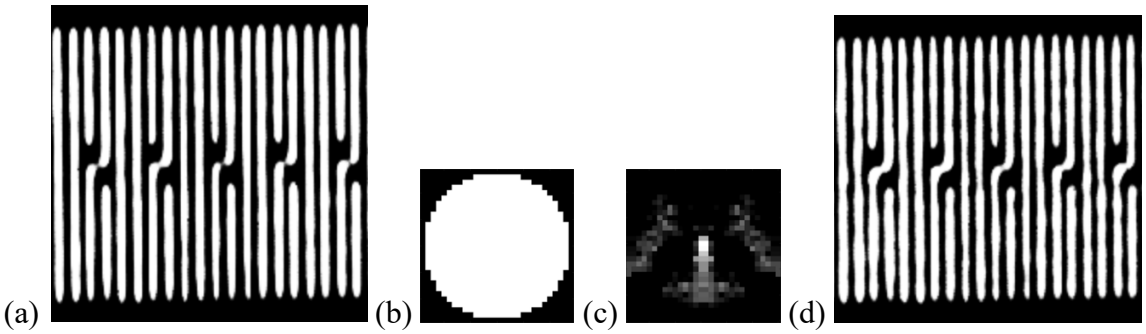


Figure 8. Aerial image of a region of interest within the 15 nm CD (1x) line ends from Figure 6, shown at a threshold (a), and corresponding pupil fill (b). Optimized source (c), and corresponding aerial image at threshold (d).

This simple demonstration is meant to illustrate the idea of source optimization using the source angular stack. There is uncertainty in the input data recorded on the mask-imaging demonstrator. It is not implied that the optimized source provides the required process window to print the pattern in question. Any real-world application of the technique would require accurate input data recorded through focus, as well as a targeted merit function to perform the optimization.

6. SUMMARY AND OUTLOOK

A mask-imaging demonstrator is commissioned at undulator beamline twelve of the Advanced Light Source. The instrument is a zoneplate-based actinic full-field EUV mask microscope similar to the SHARP microscope. The demonstrator achieves full-well exposure times below 100 milliseconds. The source angular stack is introduced as a complementary imaging mode. It contains image data recorded from up to 1500 individual illumination angles at a high framerate. Datasets can be recorded in less than 30 seconds. Data can be recorded through-focus. Synthetic images corresponding to any desired pupil fill can be computed from the stack. The imaging mode is used both on the SHARP microscope and the mask-imaging demonstrator. Fourier-Ptychographic reconstructions of the complex field of the object are demonstrated using data from the source angular stack. An example is presented, illustrating source optimization based on data from the stack. Next steps include the integration of the source angular stack with SHARP's user interface and image-processing tools, and a study to adapt the FP reconstruction algorithm to the shot-noise characteristics and angular diversity of the stack.

ACKNOWLEDGEMENTS

This work was performed by the University of California, Lawrence Berkeley National Laboratory, under the auspices of the Director, Office of Science, of the U.S. Department of Energy (Grant No. DE-AC02-05CH11231), using resources of the Advanced Light Source, which is a DOE Office of Science User Facility.

REFERENCES

[1] Markus Weiss, Dirk Hellweg, Jan Peters, et al., "Actinic review of EUV masks: first results from the AIMS EUV system integration," Proc. SPIE 9048, Extreme Ultraviolet (EUV) Lithography V, 90480X (2014). https://doi.org/10.1117/12.2046302

[2] Anna Tchikoulaeva, Hiroki Miyai, Tsunehito Kohyama, et al., "Enabling EUVL high-volume manufacturing with actinic patterned mask inspection," Proc. SPIE 11323, Extreme Ultraviolet (EUV) Lithography XI, 113231K (2020). https://doi.org/10.1117/12.2557858

[3] Patrick Naulleau, et al., "EUV Research at Berkeley Lab: Enabling Technologies and Applications," X-Ray Lasers 2014: Proceedings of the 14th International Conference on X-Ray Lasers, Springer (2015). https://doi.org/10.1007/978-3-319-19521-6_38

[4] Kevin Dorney, et al., "Actinic inspection of the extreme ultraviolet optical parameters of lithographic materials enabled by a table-top, coherent extreme ultraviolet source," Journal of Micro/Nanopatterning, Materials, and Metrology 23(4), 041406 (2024). https://doi.org/10.1117/1.JMM.23.4.041406

[5] Yasin Ekinci, Terence Garvey, Andreas Streun, et al., "A high-brightness accelerator-based EUV source for metrology applications," Proc. SPIE 10810, Photomask Technology 2018, 108100W (2018). https://doi.org/10.1117/12.2501930

[6] Kenneth A. Goldberg, Iacopo Mochi, Markus Benk, et al., "Commissioning an EUV mask microscope for lithography generations reaching 8 nm", Proc. SPIE 8679, Extreme Ultraviolet (EUV) Lithography IV, 867919 (2013). https://doi.org/10.1117/12.2011688

[7] Paul Kirkpatrick, Albert Baez, "Formation of Optical Images by X-Rays," J. Opt. Soc. Am. 38, 766-774 (1948). https://doi.org/10.1364/JOSA.38.000766

[8] Daniel Smith, "Illumination in Microlithography," Proc. SPIE 9293, International Optical Design Conference 2014, 92931G (2014). https://doi.org/10.1117/12.2074914

[9] Stuart Sherwin, Takuro Ono, Yohei Ikebe, et al. "Long-term stability of actinic metrology and EUV mask blanks," Proc. SPIE 13687, Photomask Technology 2025, 136870D (2025). https://doi.org/10.1117/12.3073446

[10] Jue-Chin Yu, Peichen Yu, and Hsueh-Yung Chao, "Fast source optimization involving quadratic line-contour objectives for the resist image," Optics Express 20 7, 8161-8174 (2012). https://doi.org/10.1364/OE.20.008161